JOURNAL OF MATERIALS SCIENCE **36** (2001) 5829–5834

Synthesis and characterization of nanocrystalline Mg_2CoH_5 obtained by mechanical alloying

J. CHEN*, H. T. TAKESHITA, D. CHARTOUNI, N. KURIYAMA, T. SAKAI
Osaka National Research Institute, AIST, MITI, 1-8-31 Midorigaoka, Ikeda, Osaka 563-8577, Japan
E-mail: junchen@onri.go.jp, j-chin@aist.go.jp

The stoichiometric mixture of $2MgH_2 + Co$ was ball milled under a hydrogen atmosphere to synthesize nanocrystalline metal hydride Mg_2CoH_5. Upon milling, the mixture was analyzed by X-ray powder diffraction (XRD) and thermal methods employing the techniques of differential scanning calorimetry (DSC), thermogravimetry (TG) and differential thermal analysis (DTA). Hydrogen absorption and desorption measured by pressure-composition-temperature (P-C-T) curves indicated that the capacity loss was small after 20 consecutive cycling tests. The enthalpies associated with hydride formation and decomposition were measured to be -69.5 and -83.2 kJ mol^{-1} H_2, respectively. At the temperatures of this study (553 to 653 K), hysteresis decreases with increasing temperature.

1. Introduction

Metal hydrides have been of steadily increasing importance for a long time owing to their technical applications [1–5]. Recently, a large number of ternary metal hydrides having the general formula $A_xM_yH_z$, in which A is an alkali or alkaline earth and M is a transition metal, have been synthesized and characterized [6, 7]. Among them, the Mg_2NiH_4 [8–10], Mg_2CoH_5 [11], and Mg_2FeH_6 [12], which have been rationalized by the 18-electron counting rules, are of significance because of their high hydrogen storage capacity (about 3.6 to 5.5 wt%). However, the transition metal-hydrogen bonds in such metal hydride complexes are stronger than that in the commercialized $LaNi_5$ system, thus making them unsuitable for most hydrogen storage applications. An effective way of improving the hydriding or dehydriding kinetics is to use the mechanical alloying (high energy ball-milling) technique [13–16]. Hydrogen storage materials, which are obtained by this method, possess various nanometer-scale nanocrystallites, showing enhanced hydrogen absorption properties over their polycrystalline counterparts e.g. mild activation conditions and lower absorption temperature [17].

It is worth noting that the mechanical alloying process has already been applied to the Mg_2Ni-H [18–21] and Mg_2Fe-H [22] systems, but not to the Mg_2Co-H. It is well known that Mg and Co do not alloy at all in the H-free solid metallic state. This is the reason why the metal hydride complex Mg_2CoH_5 is normally prepared by sintering Mg and Co powders under high hydrogen pressures. The preparation and hydrogenation properties of magnesium-cobalt hydride have been characterized. As reported by Zolliker *et al*. [11] Mg_2CoH_5 and its deuteride were prepared by sintering Mg and Co at temperatures between 620 and 720 K under a hydrogen (or deuterium) pressure of 4 to 6 MPa. These compounds are black crystalline solids with a tetragonally distorted CaF_2-type metal atom structure, which transforms at 488(5) K into a disordered cubic modification. Values of -86 and -60 kJ mol^{-1} H_2 were obtained, respectively, for the heats of dissociation and formation of Mg_2CoH_5 phase, indicating a considerable hysteresis. Ivanov *et al*. [23] measured a series of pressure-composition-isotherms and found two hydride phases Mg_2CoH_5 and Mg_3CoH_5 that had the enthalpies of -79 and -70 kJ mol^{-1} H_2 for hydrogen desorption, respectively. Yoshida *et al*. [24] estimated the enthalpies of Mg_2CoH_5 with -95 kJ mol^{-1} H_2 for lower plateau and -108 kJ mol^{-1} H_2 for upper plateau. Reiser *et al*. [25] carried out an excellent cyclic-stability test with a mixture of Mg and Co powder in an atomic ratio of 2 : 1, and calculated a heat of about $-76(4)$ kJ mol^{-1} H_2 for desorption of $Mg_6Co_2H_{11}$. From these published works, it can be seen that the hydrogen loading and cycling stability of Mg_2Co-H have been examined, however, the results were in disagreement and the equilibrium absorption pressures were not reported. Therefore, considerable issues still remain in this system, in particular regarding the effect of ball milling on its thermodynamic and dynamic properties. Herein, we are prompted to investigate the hydrogenation characteristics of Mg_2CoH_5 prepared by ball-milling the stoichiometric composition of $2MgH_2 + Co$ under a hydrogen atmosphere.

* Author to whom all correspondence should be addressed.

2. Experimental

The metal powders Mg (99.9%) and Co (99.99%) were supplied by Santoku Metal Industry Corporation. Hydride powder MgH_2, which was obtained through the reaction of Mg with hydrogen in an automatic Sieverts apparatus for several days, showed a X-ray powder diffraction pattern consistent with data listed in the JCPDS card [26]. Both the stoichiometric mixture $2MgH_2 + Co$ of 5 g and 5 steel balls of 4 mm in diameter were sealed in a vial of 100 cm^3 internal volume. The weight ratio between the powder and ball was 1 : 8. High-purity hydrogen (7N) of 0.1 MPa was introduced into the vial through a connection valve. The milling was carried out in a Kurimoto BX254E apparatus at a speed of 700 round min^{-1}, which corresponds to a maximum acceleration of 47.9 G (the gravity of the Earth), for periods from 1 to 10 h at ambient temperature. At regular intervals, a small amount of powder was taken out for analysis. All material handling (including weighing and loading) was always performed in a glove box filled with pure argon (99.999%) so as to minimize the effect of oxygen and water on the powder.

The X-ray powder diffraction (XRD) was studied on a Rigaku RU-200 system with monochromatic Cu K_α radiation operated at 40 kV with a current beam of 150 mA. Powders were mixed with a protective coating of pyrophyllite oil, smeared on a glass slide. The X-ray intensity was measured over a diffraction angle from 5 to 85° with a velocity of 0.02° per step and 2° min^{-1}. Differential scanning calorimetry (DSC) was performed using a DSC 8230HP calorimeter at a heating rate of 5 K min^{-1} under 3.0 MPa of hydrogen with the aim of determining the influence of temperature on hydrogen absorption and desorption. The thermogravimetry (TG) and differential thermal analysis (DTA) were performed employing a TG 8120 apparatus. Prior to the run, the sample (typically 20 mg) was stabilized for 10 min at 303 K and then the temperature was linearly increased to 773 K with a ramp of 5 K min^{-1} in a slow stream of argon. The microstructure was examined using a JEOL JSM-5600 scanning electron microscope equipped with an energy dispersive X-ray spectroscope (SEM-EDXS). The pressure-composition-temperature (P-C-T) curves for hydrogen absorption/desorption were determined by using an automated Sieverts-type apparatus in the fixed temperature range from 553 to 653 K and in the hydrogen pressure range from 0.01 to 3.3 MPa. The volume in the hydriding/dehydriding process had been carefully calibrated before the actual measurement. The sample holders were held in a KOYO LINDBERG furnace and the temperatures were maintained constant within 2 K at any temperature by controlling a portion of the heating current with a chromel-alumel thermocouple.

3. Results and discussion

The initial color of the $2MgH_2 + Co$ mixture was light gray. After ball milling only for 1 h, the color was dark gray. After ball milling for 2 h, the color of the powder was dark. The ball-milling process lasted for a total of 10 h, and the final powder was black in color. Fig. 1 shows the XRD patterns of the $2MgH_2 + Co$ mixture as a function of ball-milling time. Note that the phase structure has been greatly changed after ball milling. By inspection of the XRD pattern of the initial $2MgH_2 + Co$, it is easy to identify the presence of MgH_2 (marked by M) and Co, as expected. However, after only 1 h of ball milling, there is evidence of new peaks that are marked by N, indicating the formation of new phases. In addition, the peak intensities of the phases of MgH_2 and Co decrease obviously. The XRD pattern of the $2MgH_2 + Co$ mixture ball-milled for 2 h shows an increased abundance of the new phase. The MgH_2 and Co phases are seen present. After 5 h of milling, the MgH_2 and Co phases have nearly disappeared, illustrating that the initial MgH_2 phase has been basically used up to synthesize the new phase. This is confirmed by the fact that further ball milling up to 10 h does not significantly change the phase distribution. Previous studies have identified four phases in the Mg-Co-H system: tetragonal Mg_2CoH_5 [11], hexagonal Mg_3CoH_5 [23], orthorhombic $Mg_6Co_2H_{11}$ [27], and cubic $Mg_{2-x}CoH_\varepsilon$ ($\varepsilon \approx 0$) [24]. Interestingly, the d-values of the sample obtained after 10 h of ball-milling of the $2MgH_2 + Co$ are very close to those of a mixture of x-ray lines dominated by the tetragonal Mg_2CoH_5 and the hexagonal Mg_3CoH_5. In this study, a structure analysis was not attempted because of some broad peaks that are not ideal for lattice parameter determination.

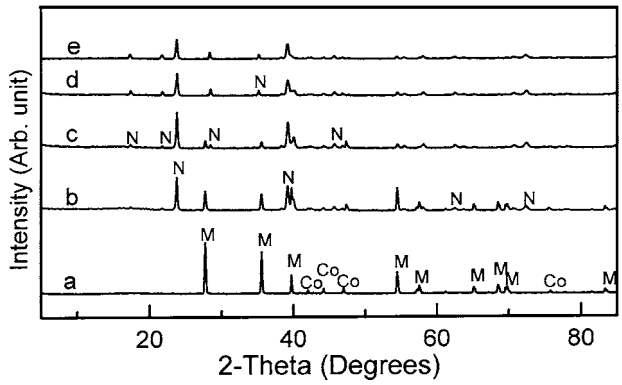

Figure 1 XRD patterns of $2MgH_2 + Co$ mixture as a function of ball milling time: (a) 0 h; (b) 1 h; (c) 2 h; (d) 5 h; and (e) 10 h. (M) MgH_2; (N) Mg-Co-hydride.

Morphological changes of the as milled powders were examined by SEM observation (Fig. 2). The particle sizes of the mixture before ball milling are in the range of 5 to 15 μm, having a smooth surface. The particles consist of visibly separated MgH_2 (the gray portion) and Co (the white portion). However, the SEM images of the powders after ball milling show rather different appearances. After 1 h of ball milling, the particles experience a rapid decrease in average size to about 2 μm with a relatively homogenous distribution of Co. By further ball milling, the element Co reacts with the MgH_2 particle to form a phase with a large surface area, evidenced by EDXS analysis. It was found that these zones contain the elements of Mg and Co, with atomic ratios of Mg: Co=1.96:1.00. This result indicates that the composition of the phase formed during ball milling is about Mg_2Co not considering the hydrogen concentration. After 5 h of ball milling, powder

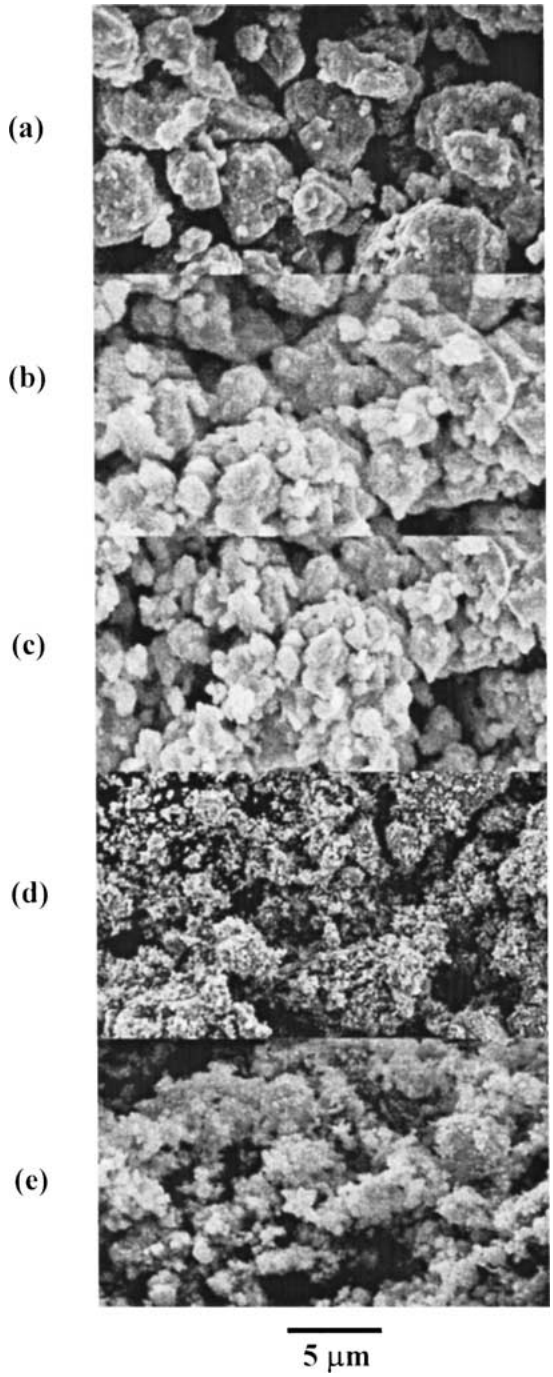

Figure 2 SEM images of $2MgH_2 + Co$ mixture during ball milling under a hydrogen atmosphere: (a) 0 h; (b) 1 h; (c) 2 h; (d) 5 h; and (e) 10 h.

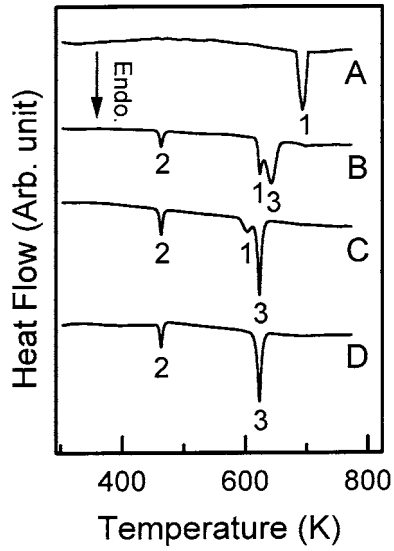

Figure 3 DSC curves: (A) initial $2MgH_2 + Co$ mixture; and ball milling for (B) 1 h; (C) 2 h; (D) 10 h.

microstructures consist of porous nanoparticles; moreover, those crystallites agglomerated such that the boundaries of individual nanocrystallines were not completely discernable. Since the "crystal" size of the final milled powder is in the range of nanometers with a highly disordered subsurface layer, it can be deduced that this sample has a huge specific surface area. The mechanism of the present mechanical alloying is dry milling of MgH_2 and Co powders in a high-energy ball mill under hydrogen atmosphere, so the MgH_2 and Co powders are repeatedly cold-welded by the colliding balls. Initially, composite powder particles with a characteristically layered microstructure (Mg_2Co-H) are formed. Subsequently, interdiffusion takes place, resulting in a strongly disordered subsurface layer. Thus, the ball-milled sample is not simply a mixture of the starting components, but a single phase Mg_2CoH_x is formed. This behavior should be favorable for hydrogen desorption and absorption of the studied Mg_2Co-H phase.

The effect of ball-milling time on the positions of the DSC peaks is illustrated in Fig. 3. The DSC heating curve of the initial $2MgH_2 + Co$ mixture (Fig. 3a) shows one sharp endothermic peak around 693 K denoted as 1 owing to the dehydrogenation of MgH_2 to Mg. Based on the area of this peak, the enthalpy change associated with the hydrogen desorption was calculated to be -72 kJ mol^{-1} H_2, which is very close to -74 kJ mol^{-1} H_2 for the decomposition of MgH_2 reported by Stampfer *et al*. [28]. However, such a DSC behavior is strongly affected by the ball-milling. As indicated in Fig. 3b and c, there are three endothermic peaks denoted as 1, 2 and 3, respectively, illustrating that new hydride phase was formed during the milling process. By further milling (Fig. 3d), peak 1 disappeared, while peak 2 and 3 still existed. Since a new hydride phase is formed at the expense of MgH_2 and since pure Co does not desorb hydrogen, peak 1 can be attributed to the thermal decomposition of MgH_2. The disappearance of this peak after 10 h of milling is in agreement with the XRD analysis as given in Fig. 1. As deduced from previous thermal analyses [11, 23], peak 2 is related to the allotropic phase transition of the new hydride, and this transformation is almost unaffected by the milling time. Peak 3 is attributed to the thermal decomposition of Mg_2Co-H, and it shifts towards lower decomposition temperature. As an example, for 10 h of milling, this peak is lowered by about 40 K relative to its position in the DSC curve after 1 h of milling. The lowering of its decomposition temperature from 693 K to 610 K should result from the increase of kinetics because the ball-milling operation leads to a phase having a high specific surface area, and possibly leads to a decrease of activation energy for dehydrogenation [29, 30]. It is noteworthy that peak 3 occurs at a higher temperature range than that of peak 1, suggesting that this phase is more stable than MgH_2.

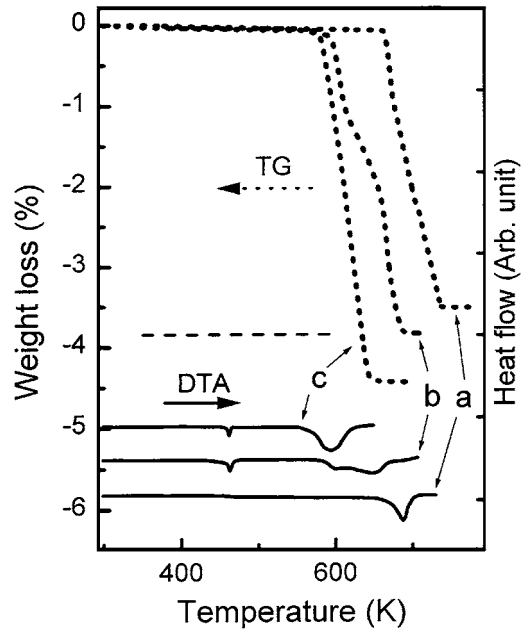

Figure 4 TG (dotted curves) and DTA (full curves) of (a) initial $2MgH_2 + Co$ mixture; and ball milling for (b) 2 h; (c) 10 h.

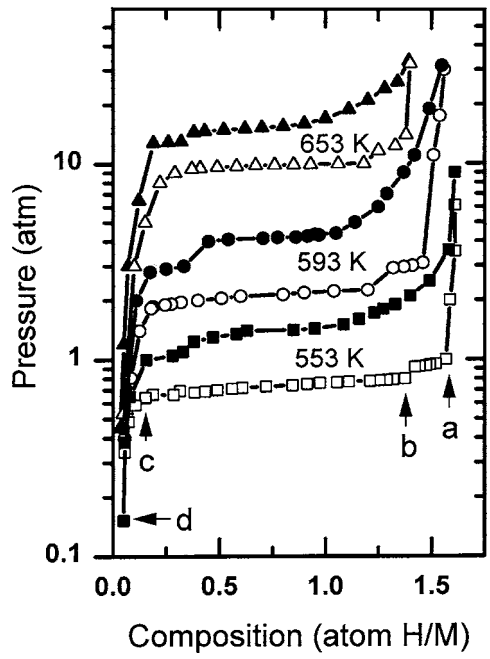

Figure 5 P-C-T curves of nanocrystalline $2MgH_2 + Co$ milled for 10 h: (open square, circle, up-triangle) desorption; (solid square, circle, up-triangle) absorption. Arrows marked by a, b, c, and d indicate examined XRD patterns that are shown in Fig. 7.

Fig. 4 shows the thermal analyses (TG and DTA) of the $2MgH_2 + Co$ with the change of ball-milling time. It is obvious that both the dehydriding and thermal reactions are rather different among the three samples analyzed. The results of TG analysis indicate that the hydrogen content increases with increasing ball-milling time owing to absorption of hydrogen by the starting $2MgH_2 + Co$; whereas the DTA data reveal that the starting temperature of the dehydriding reaction shifts to lower temperature with increasing ball-milling time, resulting from the changes of kinetic factors such as the surface characteristics of the milled particles. In the case of the initial mixture, there is one weight loss in the TG profile and one endothermic reaction in the DTA profile. The desorption of hydrogen starts at 650 K and ends at 740 K, giving a total loss value of 3.5 weight % H_2. The endothermic reaction is attributed to the dehydriding reaction of the MgH_2 to Mg. In the case of the sample after 2 h of ball milling, there are two obvious weight losses in the TG curve and three endothermic reactions in the DTA curve. The starting temperature of hydrogen desorption is around 590 K, and the dehydriding reaction is completed at 700 K, reaching a value of 3.8 wt%. The endothermic peak at 460 K confirms the allotropic phase transition of the Mg_2Co-hydride phase as mentioned in DSC analysis of Fig. 3. Here, we will focus on the two endothermic peaks around 590 and 640 K. Owing to the small content of MgH_2 coexisting in the milled sample, the former one could be attributed to the dehydrogenation of MgH_2, while the latter corresponds to the decomposition of Mg_2Co-hydride. Note that the peak for MgH_2 desorption is lowered by about 50 K in comparison with the profile of the initial hydride. For the sample after 10 h of ball milling, the dehydriding reaction begins at around 580 K and ends at 650 K, reaching higher hydrogen content of 4.4 wt%. The DTA results show that two endotherms are observed, one at 460 K and a slightly more intensive endotherm at 590 K, meaning that all the MgH_2 has been transformed into the Mg_2Co-hydride. The maximum hydrogen content of 4.4 wt% obtained in this study is nearly the same as that in the formula unit of Mg_2CoH_5 (4.5 wt%). Combining the results obtained through XRD, SEM and DSC, it is thus deduced that the Mg_2Co-hydride is Mg_2CoH_5.

The stability of the sample after 10 h of ball milling was characterized through P-C-T measurements. Fig. 5 shows the representative curves at 553, 593, and 653 K. There exist two plateau regions corresponding to either the absorption or the desorption data. At any temperature, the lower plateau on the absorption side corresponds to the conversion of Mg to MgH_2, whereas the upper one on the desorption side is due to the decomposition of MgH_2. However, the upper plateau on the absorption curve and the lower plateau on the desorption side result from hydriding of $Mg_xCo + Mg + Co$ and dehydriding of ternary Mg_2CoH_5. From the plateau length, one can estimate that the phase abundance of the Mg_2CoH_5 is much higher than that of MgH_2. The two plateaus reported for ternary Mg-Co-hydride [11, 23–25] were not observed in our data, only one sloping plateau except that MgH_2 was observed. The different synthesis method and the various measurements of temperature range between the present study and literature work could explain this difference. Furthermore, it can be seen that the equilibrium hydrogen pressures for hydrogen absorption (P_{abs}) are greater than for hydrogen desorption (P_{des}). This is the phenomenon known as hysteresis [31]. Table I summarizes the plateau pressures as well as the hysteresis factor ($\ln(P_{abs}/P_{des})$) for the studied Mg_2CoH_5. As can be seen from those data, hysteresis decreased with increasing temperature owing to the smaller free energy loss at higher temperatures. It is known that the time-independent plateau pressures for hydride formation or decomposition are affected by the irreversible

TABLE I Plateau pressures for hydrogen absorption and desorption (P_{abs} and P_{des}) as well as the hysteresis factor ($\ln(P_{abs}/P_{des})$ for the studied Mg_2CoH_5

Temperature (K)	P_{abs} (atm)	P_{des} (atm)	$\ln(P_{abs}/P_{des})$
553	1.6	0.65	0.90
593	4.5	2.10	0.76
653	16.0	10.2	0.45

TABLE II Thermodynamic parameters of the prepared sample for hydrogen absorption (abs) and desorption (des)

	ΔH (kJ mol^{-1} H_2)		ΔS (J mol^{-1} K H_2)	
Composition	Abs	Des	Abs	Des
Mg_2CoH_5	−69.5	−83.2	−129.6	−146.7
MgH_2	−68.4	−74.5	−124.2	−134.0

dissipation of free energy which may contain contributions from plastic deformation, hydrogen dissociation and hydride (metal) nucleation processes [32]. At higher temperatures, the less the energy dissipation, the lower the plateau pressure for hydride formation and the higher the plateau pressure for hydride decomposition, and thus the smaller the hysteresis.

The Van't Hoff plot is a convenient way to obtain the thermodynamic parameters that can be used to compare hydrides of varying stability. Based on the plateau pressures at different temperatures listed in Table I, a plot of $\ln P$ vs. $1/T$, given in Fig. 6. The plot can be fitted by a straight line with its slope being a measure of enthalpy (ΔH) and the intercept a measure of entropy (ΔS). The obtained values are summarized in Table II. The ΔH and ΔS are negative, meaning the hydriding reaction is exothermic and the dehydriding reaction is endothermic. The ΔH values derived from the shorter plateaus for absorption and desorption are −68.4 and −74.5 kJ mol^{-1} H_2, respectively. The latter is in good agreement with previous values obtained by Stampfer *et al*. [28] and Reilly *et al*. [33] confirming that the higher plateau on desorption corresponds to dehydriding of MgH_2 and that the analyses of DSC, TG and DTA mentioned above are correct. Similarly, the ΔH values from the longer plateaus are −69.5 kJ mol^{-1} H_2 (absorption) and −83.2 kJ mol^{-1} H_2 (desorption). Those values agree well with reported data of such systems, indicating that the strength of M-H bonding in these ternary hydrides is almost the same. Moreover, the ternary hydride shows higher value of ΔH (absolute) than that of MgH_2, suggesting this hydride is more stable. The above results indicate the ball milling technique is very useful in synthesizing the stable hydride Mg_2CoH_5 directly at room temperature rather than by sintering at high hydrogen pressures and high temperatures.

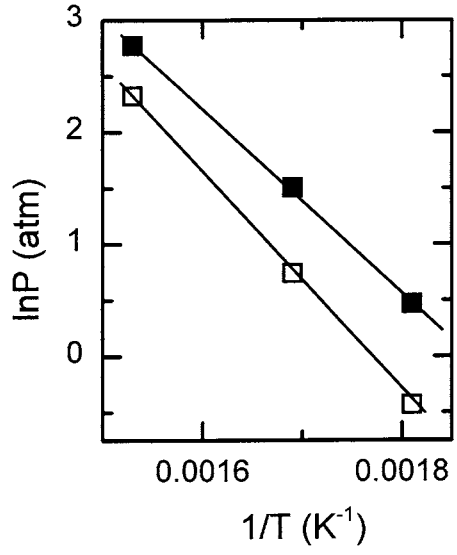

Figure 6 The Van't Hoff plot for the detected Mg_2CoH_5: (solid square) absorption; (open square) desorption.

In this work, no extensive cycling test has been carried out. The hydrogen uptake of the sample decreased by only 2% after a preliminay test to 20 consecutive cycles of absorption and desorption. This result shows that the fine microstructures help to maintain favorable absorption/desorption characteristics. It is interesting to note that Mg_2CoH_5 decomposes in a particularly interesting step. Considering the small amount of coexisting MgH_2, it is believed that the desorption corresponds to the following reactions

$$MgH_2 \rightarrow Mg + H_2 \quad (1)$$

$$Mg_2CoH_5 \rightarrow Mg_xCo + Mg + Co + H_2 \quad (2)$$

and Equations 1 and 2 can be confirmed from the XRD spectra of Mg_2CoH_x at different values of x, as shown in Fig. 7. The value of x was estimated from the corresponding PCT curves. The upper spectrum is for the fully hydrided sample Mg_2CoH_5, and the peaks are quite similar to those of the monoclinic phase as mentioned in Fig. 1 for $2MgH_2 + Co$ after 10 h of ball milling. The second spectrum (Fig. 7b) shows the appearance of new peaks which can be attributed to pure magnesium. These new peaks are from the decomposition of MgH_2 to Mg, and the fine particles of Mg have agglomerated and fused together to form larger grain sizes. Comparing Mg_2CoH_1 with Mg_2CoH_4, we observed growth of an alloy phase and an increase of Mg content at the expense of the monoclinic hydride phase. The alloy phase is marked by X, in particular at the two-theta angles around 13 and 22.5°. With the complete desorption of hydrogen, the peaks of the bottom spectrum showed evidence of the presence of the alloy phase as well as Mg and Co. It is pointed out that

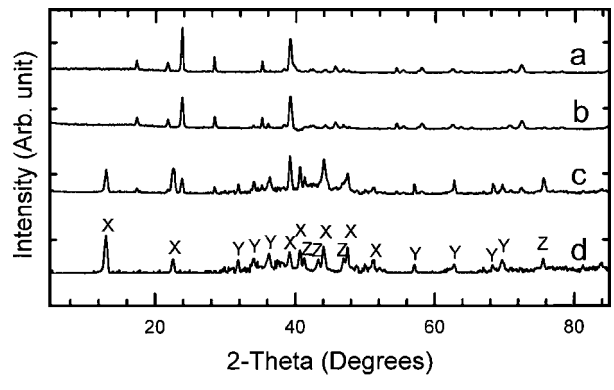

Figure 7 XRD patterns of Mg_2CoH_x for different values of x that are estimated from P-C-T curves as marked in Fig. 5: (a) $x = 5$; (b) $x = 4$; (c) $x = 1$; and (d) $x \approx 0$. (X) Mg_xCo; (Y) Mg; (Z) Co.

the color of Mg_2CoH_5 and Mg_2CoH_4 is black, while that of Mg_2CoH_1 and $Mg_2CoH_{\approx 0}$ is gray. When the resultant was hydrided by saturating with hydrogen, the XRD pattern of the residue showed similar phases as presented in Fig. 7a. Thus, on the basis of X-ray studies, reactions 1 and 2 in the plateau regions are reversible. The existence of Mg_2Co phase has been previously reported [23], with a face-centered cubic cell ($a = 11.43(1)$ Å) [34]. In this study, however it is not possible to determine the crystal structure of the pure alloy (or with little hydrogen) phase because of the difficulty of separating the alloy phase from the others. To illustrate this satisfactorily, a detailed study would be required to verify the alloy phase formed.

The above experimental results prove that mechanical alloying of MgH_2 and Co crystalline powders produces the intermetallic phase Mg_2CoH_5 by milling at a high intensity. This shows a new way for the synthesis of Mg_2CoH_5 by milling directly starting from a mixture of MgH_2 and Co. To our knowledge, the reversible hydrogen content of 4.4 wt% in Mg_2CoH_5 presented in this work can be obtained at the relatively low temperature of 553 K, which is the lowest temperature reported for this system, giving potential to this material as a hydrogen storage medium.

4. Conclusions

The ternary hydride Mg_2CoH_5 was synthesized by ball milling the mixture $2MgH_2 + Co$ under a hydrogen atmosphere. This denoted an improvement in the kinetics of hydride formation. The sample as prepared by the milling technique showed the characteristics of nanocrystalline structure with a high specific surface. The thermal analysis study indicated that the decomposition temperatures for MgH_2 and Mg_2CoH_5 were reduced owing to their very fine microstructure. The sample showed rapid dissociation and uptake of hydrogen at 3 MPa, indicating that the cobalt milling was thus playing a very active role at the alloy/hydride surface in dissociating hydrogen and so enabling more rapid hydride formation via the metastable phase. The enthalpies relating to the dissociation and formation of Mg_2CoH_5, which were based on pressure-composition-temperature curves, were -83.2 and -69.5 kJ mol^{-1} H_2, respectively. X-ray diffraction results appear to confirm that in the desorption step, the Mg_2CoH_5 decomposes to $Mg_xCo + Mg + Co + H_2$ where x is around 2, while in the absorption process it is reversible. After 20 consecutive cycles at 553 K, the hydriding capacity loss was only 2% and the hysteresis value ($\ln(P_{abs.}/P_{des.})$) was 0.90.

Acknowledgement

This work was financially supported by the New Energy and Industrial Technology Development Organization (NEDO) and carried out under the World Energy Network (WE-NET) Project - International Clean Energy Technology Utilizing Hydrogen.

References

1. D. G. IVEY and D. O. NORTHWOOD, *J. Mater. Sci.* **18** (1983) 321.
2. L. SCHLAPBACH, in "Hydrogen in Intermetallic Compounds I & II" (Springer-Verlag, Berlin, 1988, 1992).
3. G. G. LIBOWITZ, in "Hydrogen Storage Materials, Batteries, and Electrochemistry," edited by D. A. Corrigan and S. Srinivasan (The Electrochemical Society, Pennington, 1992) p. 3.
4. T. SAKAI, M. MATSUOKA and C. IWAKURA, in "Handbook on the Physics and Chemistry of Rare Earths," edited by K. A. Gschneidner, Jr. and L. Eyring (Elsevier Science B.V., Amsterdam, 1995) Vol. 21, p. 133.
5. G. SANDROCK and G. THOMAS, *IEA/DOE/SNL Hydride Databases*, Internet URL http://hydrpark.ca.sandia.gov.
6. T. K. FIRMAN and C. R. LANDIS, *J. Am. Chem. Soc.* **120** (1998) 12650.
7. M. OLOFSSON-MÅRTENSSON, M. KRITIKOS and D. NORÉUS, *ibid.* **121** (1999) 10908.
8. J. J. REILLY and R. H. WISWALL, JR., *Inorg. Chem.* **7** (1968) 2254.
9. D. NORÉUS and L. G. OLSSON, *J. Chem. Phys.* **78** (1983) 2419.
10. Z. GAVRA, G. KIMMEL, Y. GEFEN and M. H. MINTZ, *J. Appl. Phys.* **57** (1985) 4548.
11. P. ZOLLIKER, K. YVON, P. FISCHER and J. SCHEFER, *Inorg. Chem.* **24** (1985) 4177.
12. J. J. DIDISHEIM, P. ZOLLIKER, K. YVON, P. FISCHER, J. SCHEFER, M. GUBELMANN and A. F. WILLIAMS, *ibid.* **23** (1984) 1953.
13. L. ZALUSKI, P. TESSIER, D. H. RYAN, C. B. DONER, A. ZALUSKA, J. O. STRÖM-OLSEN, M. L. TRUDEAU and R. SCHULZ, *J. Mater. Res.* **8** (1993) 3059.
14. L. ZALUSKI, A. ZALUSKA, P. TESSIER, J. O. STRÖM-OLSEN and R. SCHULZ, *J. Alloys Comp.* **217** (1995) 295.
15. J. CHEN, D. H. BRADHURST, S. X. DOU and H. K. LIU, *J. Mater. Sci.* **33** (1998) 4671.
16. E. AKIBA, *Current Opinion in Solid State & Mater. Sci.* **4** (1999) 267.
17. S. ORIMO, H. FUJII and K. IKEDA, *Acta Mater.* **45** (1997) 331.
18. Y. Q. LEI, Y. M. WU, Q. M. YANG, J. WU and Q. D. WANG, *Z. Phys. Chem.* **183** (1994) 379.
19. J. HOUT, E. AKIBA and T. TAKADA, *J. Alloys Comp.* **231** (1995) 815.
20. C. IWAKURA, S. NOHARA, H. INOUE and Y. FUKUMOTO, *Chem. Commun.* (1996) 1831.
21. T. KOHNO and M. KANDA, *J. Electrochem. Soc.* **144** (1997) 2384.
22. J. HOUT, S. BOILY, E. AKIBA and R. SCHULZ, *J. Alloys Comp.* **280** (1998) 306.
23. E. J. IVANOV, I. KONSTANCHUK, A. STEPANOV, J. YAN, M. PEZAT and B. DARRIET, *Inorg. Chem.* **28** (1989) 613.
24. M. YOSHIDA, F. BONHOMME, K. YVON and P. FISHER, *J. Alloys Comp.* **190** (1993) L45.
25. A. REISER, B. BOGDANOVIC and K. SCHLICHTE, *Int. J. Hydrogen Energy* **25** (2000) 425.
26. JCPDS Card No. 12-697 (MgH_2) (JCPDS-ICDD, Newtown Square, PA19073, 1999).
27. R. CERNY, F. BONHOMME, K. YVON, P. FISHER, P. ZOLLIKER, D. E. COX and A. HEWAT, *J. Alloys Comp.* **187** (1992) 233.
28. J. F. STAMPFER, JR., C. E. HOLLEY, JR. and J. F. SUTTLE, *J. Am. Chem. Soc.* **82** (1960) 3504.
29. S. TANAKA, J. D. CLEWLEY and T. B. FLANAGAN, *J. Phys. Chem.* **81** (1977) 1684.
30. K. FOSTER, R. G. LEISURE, J. B. SHAKLEE, J. Y. KIM and K. F. KELTON, *Phys. Rev. B* **61** (2000) 241.
31. G. SANDROCK, *J. Alloys Comp.* **293–295** (1999) 877.
32. S. QIAN and D. O. NORTHWOOD, *Int. J. Hydrogen Energy* **13** (1988) 25.
33. J. J. REILLY and R. H. WISWALL, JR., *Inorg. Chem.* **6** (1967) 2220.
34. E. M. CRAMER, H. P. NIELSEN and F. W. SCHONFELD, *Light Met. Age* **5** (1947) 6.

Received 19 October 2000
and accepted 9 July 2001